Journal of Membrane Science 348 (2010) 1–5

Contents lists available at ScienceDirect

Journal of Membrane Science

journal homepage: www.elsevier.com/locate/memsci

Rapid communication

Robust method for micro-porous silica membrane fabrication

M.W.J. Luiten*, Nieck E. Benes, Cindy Huiskes, Henk Kruidhof, Arian Nijmeijer

Inorganic Membranes, Department of Science and Technology and MESA+ Institute for Nanotechnology, University of Twente, P.O. Box 217, 7500 AE Enschede, The Netherlands

ARTICLE INFO

Article history:
Received 27 August 2009
Received in revised form 5 November 2009
Accepted 14 November 2009

Keywords:
Gas separation
Silica
Tubular membrane
Hydrogen
Thermal stability

ABSTRACT

High performance large surface area micro-porous silica membranes have been prepared using a robust method that combines reduced roughness of the membrane support surface with a straightforward coating procedure. The method allows for reproducible production of membranes with a flat plate or tubular geometry. Tubular membranes with a length suitable for commercial application (55 cm) show performance comparable, in terms of flux and permselectivity, to that of low surface area flat plate membranes and shorter tubes (10 cm). At 250 °C and pressure difference of 2 bar the hydrogen permeance of the 55 cm membranes is in the range $(0.5–1) \times 10^{-6}$ mol m^{-2} s^{-1} Pa^{-1}, and the permselectivity of hydrogen with respect to methane is in the range 350–400. Permeation measurements below 400 °C over a period of more than 2100 h showed no significant changes in permeance or permselectivity.

1. Introduction

Micro-porous silica membranes have been studied for decennia. These membranes can be highly selective for small gases at higher temperatures and are potentially interesting for applications involving selective removal of hydrogen. Applications with commercial prospective include the water–gas shift reaction and equilibrium-restricted processes such as dehydrogenation [1]. For commercial application silica membranes with tubular or hollow fiber geometry seem most promising. An overview of relevant publications related to silica membranes with such geometries is listed in Table 1.

The table shows that CVD and sol–gel chemistry combined with a coating technique prevail for silica membrane fabrication. Membranes prepared via CVD display high permselectivity for hydrogen over nitrogen or methane, combined with low hydrogen permeance ($(1–10) \times 10^{-8}$ mol m^{-2} s^{-2} Pa^{-1}). The CVD method has only been reported for limited membrane surface area, i.e., tubes with maximum length of 3–10 cm. In contrast, sol–gel derived membranes with larger surface area have been reported, i.e., tubes with a length up to 100 cm. Sol–gel chemistry is also an inherently versatile method for the production of metal oxide materials containing pores of molecular dimensions, via hydrolysis and subsequent polycondensation of precursor molecules. The interested reader is referred to for instance the book of Brinker and Scherer [17].

As compared to the CVD method the hydrogen permeance of sol–gel derived membranes is higher ($(1–10) \times 10^{-7}$ mol m^{-2} s^{-1} Pa^{-1}), but the permselectivity for hydrogen over gases with higher kinetic diameter generally lower.

The superior hydrogen flux of sol–gel derived silica membranes results from the presence of a very thin (generally <100 nm) distinct selective silica layer produced during the coating step. Although this thin layer allows for a low resistance to mass transport, the selectivity it provides is very susceptible to defects introduced during fabrication, for instance via contaminants such as dust particles. Clean-room facilities can be used to minimize contamination, however, the high costs involved form a major hurdle for economically viable fabrication of large membrane surface area. Another drawback associated with the standard sol–gel derived silica membranes is their moderate (hydro)thermal stability, limiting their use in applications involving harsh conditions.

In this work we propose a fast, straightforward, and robust method for fabrication of large surface area silica membranes with enhanced (hydro)thermal stability. The method involves the use of a closed system of communicating vessels, for coating the modified surface on the inside of a tubular support.

Fig. 1 shows a schematic representation of the coating set-up. Due to the principle of communicating vessels the height of the liquid in the membrane module is directly related to the vertical position of the feed vessel. Coating is performed by moving the feed vessel with a controlled speed in vertical direction, such that the membrane tube is first filled and subsequently emptied. After this procedure a thin film of the coating solution remains on the inside of the tube. To reduce the probability of contamination, coating is performed in a system that is completely closed from the sur-

* Corresponding author. Tel.: +31 53 489 2914; fax: +31 53 489 4611.
E-mail address: m.w.j.luiten@utwente.nl (M.W.J. Luiten).

0376-7388/$ – see front matter © 2009 Elsevier B.V. All rights reserved.
doi:10.1016/j.memsci.2009.11.029

Table 1
An overview of relevant publications related to state-of-the-art silica membranes with tubular or hollow fiber geometry.

Fabrication method	Times	Membrane length [cm]	Gas components [A/B]	Permeance P_A [mol m^{-2} s^{-1} Pa^{-1}]	Permselectivity	Measurement temperature [°C]	Institute
CVD	1	10	H_2/N_2	3.0×10^{-7}	1000	600	Kyushu University [1]
CVD	1	3	H_2/N_2	9.0×10^{-7}	50	600	Korea Inst. of Energy Research [2]
CVD	1	5	H_2/N_2	4.9×10^{-8}	2900	600	University of Tokyo [3]
CVD	1	4	H_2/CH_4	5.0×10^{-7}	5900	600	Virginia University [4]
Sol–gel wet cloth	Several	9	H_2/N_2		25–500	500	Hiroshima University [5]
Sol–gel wet cloth	Several	25	H_2/CH_4	1.3×10^{-6}	150	300	Hiroshima University [6]
	Several	1.5	H_2/N_2	2.1×10^{-7}	100	400	Kyushu University [7]
Sol–gel dip coating	4	17	He/N_2	2.2×10^{-6}	100–1000	200	Eindhoven University of Technology [8]
Sol–gel dip coating	?	40–50	H_2/N_2	2.0×10^{-5}	102	600	Noritake Company [9]
Sol–gel dip coating	?	100	H_2/CH_4	1.6×10^{-6}	28	<600	Nat.Tech. University of Athens [10]
Sol–gel dip coating	2	5.5	H_2/N_2		320	80	University of new México [11]
Sol–gel Hot coating	Several	9	H_2/N_2	9.1×10^{-8}	190	500	Hiroshima University [12]

roundings, under nitrogen. This procedure avoids the requirement of clean-room facilities.

The intermediate γ-alumina layer is doped with lanthanum to prevent pore growth as a result of the phase transformation to α-alumina [13]. To prevent delamination mono-aluminum phosphate (MAP) is used as a ceramic bonding between the α-alumina support and γ-alumina intermediate layer [14]. Membranes with different dimensions have been prepared and their single gas permeation performance has been compared with that of state-of-the-art silica membranes reported in literature.

2. Experimental

2.1. Materials

Tubes of α-alumina (length 55 cm, internal diameter 0.7 cm) with improved surface morphology were purchased from Pervatech (Netherlands). Mono-aluminum phosphate (MAP, $Al(H_2PO_4)_3$) (Alfa Aesar, 50 wt.% solution) was diluted 10 times with water. Lanthanum nitrate hexahydrate, tetraethyl orthosilicate (TEOS), and aluminum tri-sec-butylate (AlTSB) were purchased from Merck and stored in a nitrogen glove box to prevent reactions with water. Polyvinyl alcohol (PVA) (86.7–88.7 mol% hydrolysis, M_w ~67,000) was purchased from Aldrich. The chemicals were not treated prior to use, but used as received.

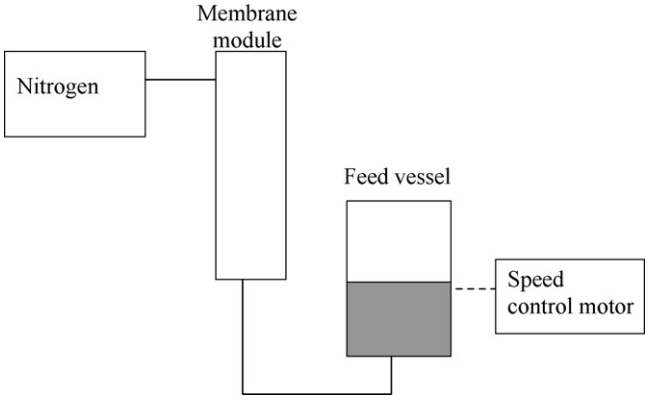

Fig. 1. Schematic diagram of the coating set-up.

2.2. Sol synthesis

Boehmite sols (γ-AlOOH) were synthesized using AlTSB as precursor [15]. For membranes with enhanced (hydro)thermal stability the boehmite was doped with 6% lanthanum [13], by thoroughly mixing the appropriate amounts of a lanthanum nitrate solution and boehmite sol. Coating solutions were obtained by mixing 30 ml boehmite sol with 20 ml PVA solution (30 g PVA/L in 0.05 M HNO_3).

Polymeric silica sols were prepared by acid-catalyzed hydrolysis and condensation of TEOS, as described in detail by de Vos and Verweij [16].

2.3. Coating procedure

Fig. 2 schematically depicts the membrane fabrication method. A glass seal was applied to the tubular tubes. The resulting tubes were coated by using a communicating vessel system, followed by calcining after each coating step, which is described in the next paragraph. All steps were carried out under clean-room conditions.

The tubes were brought in contact with the boehmite coating solution for 3 min (filling/emptying at 1.7 cm s^{-1}). The coating was repeated once, with a shorter contact time (30 s). The resulting tubes were brought in contact with the silica coating solution for 10 s (filling at 2.5 cm s^{-1}, emptying at 0.25 cm s^{-1}). The coating procedure was repeated once.

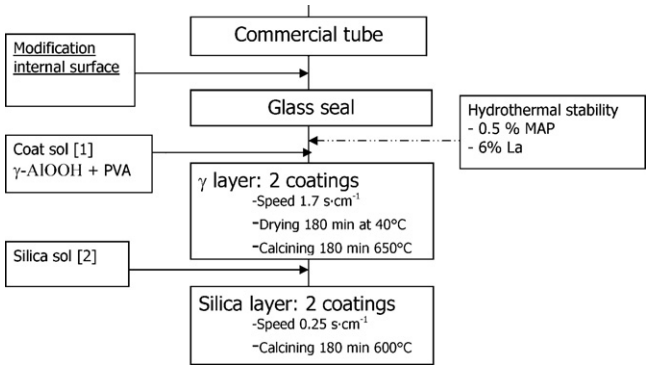

Fig. 2. Schematic representation of the fabrication method of tubular membranes.

Table 2
Layer thickness as a function of coating parameters, determined from XPS analysis.

Preparation sample			XPS profile	
Sample nr	Coating speed [cm s^{-1}]	Sol concentration [10^{-1} mol L^{-1}]	Layer thickness [nm]	Thickness layer SiO_2 intruded in Al_2O_3 [nm]
1	0.25	1.8	22	65
3	0.6	0.9	22	87
5	0.6	1.8	43	109
7	0.25	0.9	0	43

For membranes with intended enhanced (hydro)thermal stability the same coating procedure was used, preceded by an initial coating step with MAP-solution for 10 s (filling/emptying at 1.7 cm s^{-1}) and lanthanum doping of the boehmite sol.

For comparison, flat supports were coated with a rotating dip-coater (rotating speed = 1.4 cm s^{-1} for all coating solutions) with the same coating solutions.

2.4. Calcining procedures

The MAP treated alumina tubes were dried at 40 °C and 60% relative humidity for 3 h, followed by firing at 300 °C in air for 1 h (heating/cooling rate 1 °C min^{-1}).

At 40 °C and 60% humidity the γ-Al_2O_3 layers were dried for 3 h and calcined in air at a temperature of 650 °C for 3 h (heating/cooling rate 1 °C min^{-1}). Directly after coating, silica layers were calcined in air at a temperature of 600 °C for 3 h (heating/cooling rate 0.5 °C min^{-1}).

2.5. Characterization

At different longitudinal positions on the inside of the 55 cm long tubular silica membranes SEM pictures were taken of the cross-section (Zeiss 1550 High Resolution SEM, at 1.5 kV).

Single gas permeation of flat plates and tubes was measured in a pressure controlled dead-end set-up. The measurements were performed at different temperatures (T = 150–450 °C), pressures (Δp = 1–4 bar and $p_{permeate}$ = 1 atm) and for gasses (helium, hydrogen, carbon-dioxide, nitrogen, oxygen and methane). Prior to the measurements, the membranes were pretreated by permeating He or H_2 at 200 °C for 1 night. The single gas permeance F was calculated from:

$$F = \frac{N}{\Delta P}$$

where N is the molar flux through the membrane. The permselectivity F_α for a gas i with respect to a gas j was calculated from the ratio of single gas permeances:

$$F_\alpha = \frac{F_i}{F_j}$$

To investigate the long term stability of the membranes, single gas measurements were conducted over a period of 2900 h.

Gas mixture separation measurements were performed in a pressurized cross-flow cell at 250 °C (retentate flow = 45.8 L h^{-1} consisted of 89% H_2 and 11% CH_4, sweep flow = 3.2 L h^{-1} N_2, permeate pressure = 1.45 bar). Gas selectivity for H_2 with respect to CH_4 was calculated from:

$$\alpha_{H_2/CH_4} = \left(\frac{x_{H_2}}{x_{CH_4}}\right)_{permeate} \cdot \left(\frac{x_{CH_4}}{x_{H_2}}\right)_{retentate}$$

where x is the mol fraction.

3. Results and discussion

Fig. 3 depicts a typical stack of layers comprised in the tubular membranes. A distinct interface is present between the γ-alumina intermediate layer (thickness 3 μm) and the silica top layer (30 nm thick). The variation in silica layer thickness measured at different longitudinal positions in the tubes was within experimental error. As compared to flat supports prepared in this work and by others [16] the silica layer thickness of the tubular membranes was comparable, although different coating systems were used.

The influence of the coating speed and concentration of the coat sol on the silica top layer was measured in another experiment and the results are depicted in Table 2. The table shows that the silica layer thickness increases with increasing coating speed and increasing sol concentration.

Measurement at both ends of the tube shows no correlation between layer thickness and contact time, as the difference in layer thickness is within experimental error whereas the contact time at these locations is 10 and 220 s, respectively.

These observations suggest that the layer formation occurs via the dip coating process [17,18] and capillary suction of the substrate has minor influence on the thickness of the layer. During dip coating, the withdrawal speed influences the amount of sol which can flow back into the meniscus during coating; a slower coating speed creates thinner layers.

In Fig. 4, single gas permeance data (T = 250 °C, Δp = 2 bar) are presented as a function of the kinetic diameter of the permeating molecules for the different support geometries (flat, short, and long tubes). The observed trend, i.e., a high permeance for small molecules and a sharp decrease in permeance for larger molecules, is typical for micro-porous silica membranes. The performance of the tubular membranes is comparable to that of the on laboratory scale made flat plate membranes (ø = 39 cm) studied by de Vos and Verweij [16], notwithstanding that the surface area is 1000 times larger.

The data in Fig. 4 indicate variations in permeation between the different samples. For each of the gases studied the change in per-

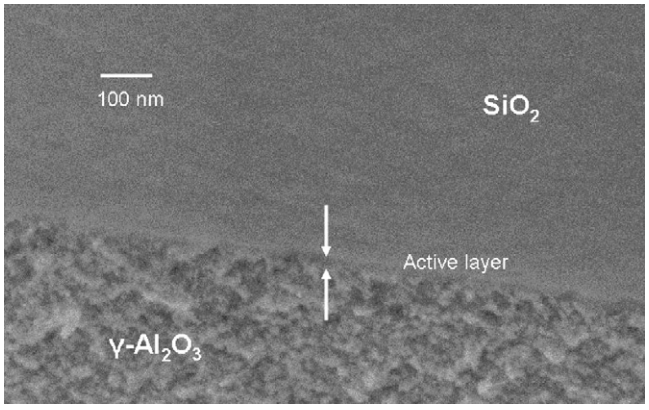

Fig. 3. SEM images showing a cross-section of silica top layer taken at the outer end of a 55 cm tubular membrane.

Table 3
Permeance, permselectivity, and selectivity of tubular silica membranes, $T = 250\,^{\circ}C$, $\Delta p = 2$ bar.

Tubular membrane 10 cm	F_α H_2/CH_4	H_2 permeance [10^{-7} mol m^{-2} s^{-1} Pa^{-1}]	Tubular membrane 55 cm	F_α He/CH_4	He permeance [10^{-7} mol m^{-2} s^{-1} Pa^{-1}]	α H_2/CH_4	H_2 permeance [10^{-7} mol m^{-2} s^{-1} Pa^{-1}]
A	420	10	F	400	11		
B	490	10	G	370	6.4		
C	190	10	H			350	4.7
D	110	10	I			360	5.1
E	660	6					

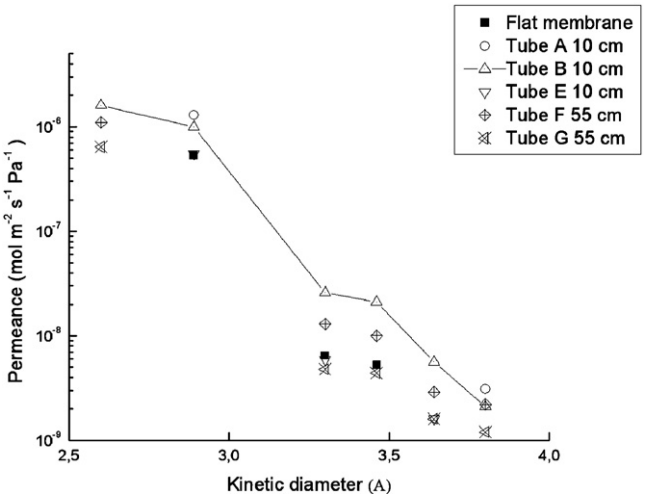

Fig. 4. Permeance as function of kinetic diameter, line is a guide to the eye.

meance per sample is similar. Consequently, permselectivity does not vary significantly between the different samples.

Table 3 shows gas permeation data of 9 tubes. For both 10 cm as well as 55 cm long tubes hydrogen permeance is in the range $(0.5–1) \times 10^{-6}$ mol m^{-2} s^{-1} Pa^{-1}. Tubes F and G (length 55 cm) display an average permselectivity, F_α, of ~390 for helium of methane. The gas separation selectivity of hydrogen over methane, α, of the other 55 cm tubes (H and I) is in the same range (~350). The performance of tubes A, B and E (10 cm) is comparable to that of the 55 cm tubes. The permselectivity of tubes C and D (10 cm) is lower. These tubes show a higher methane permeance ($(0.5–1) \times 10^{-8}$ mol m^{-2} s^{-1} Pa^{-1}), possibly due to leakage of the glass sealing. The effect of leakage is more pronounced for the shorter tubes, because of the 5 times lower membrane surface area.

For membranes with a lanthanum doped γ-alumina layer and MAP bonding prolonged performance was tested in a single gas dead-end gas permeation set-up for a total duration of 2900 h (Fig. 5).

In the first 2100 h the permeance was measured at temperatures up to 350 °C with different gases at different pressures. Fig. 5 shows the permeation data of hydrogen, methane and carbon-dioxide of tube B in time at a pressure difference of 3.8 bar. Permeance of the different gases did not vary significantly in time. Between 2100 and 2500 h the maximum temperature of the measurement was increased to 400 and 450 °C. The final gas permeance data, obtained after 2500 h, shows that membrane properties have changed irreversibly at temperatures >350 °C; a minor increase in permeance of hydrogen is observed, whereas permeance of methane (measured at 250 °C) increases 115%. The activation energy E_a for transport of hydrogen decreases from 19 to 6.3 kJ mol^{-1}. The changes in selectivity and activation energy suggest that after prolonged exposure to high temperature the pore morphology of the silica has changed and an increased number of larger pores are present. The change in pore morphology is not unexpected, given the inherent non-equilibrium nature of this amorphous material. The changes in materials properties at temperatures that are low as compared to the calcination temperature of 600 °C appear to be related to the

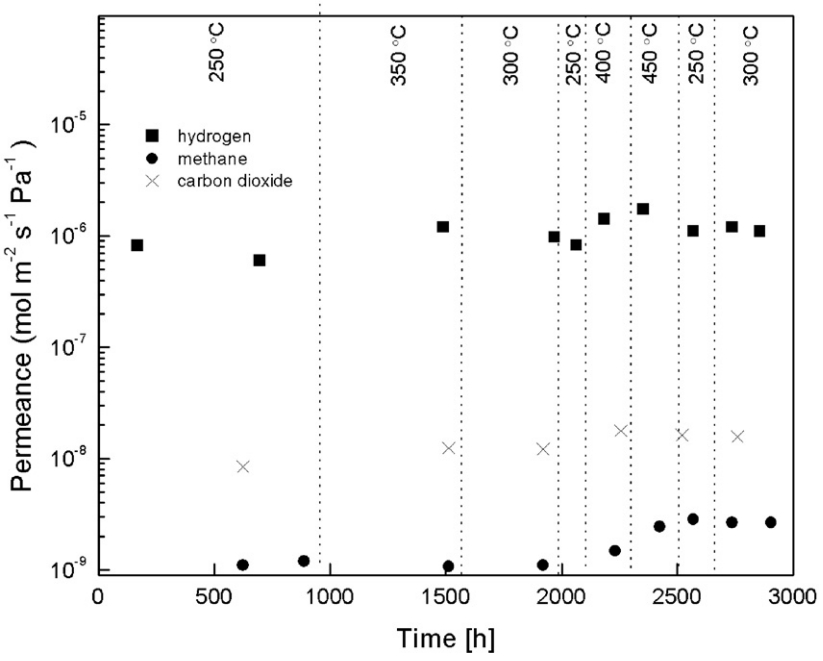

Fig. 5. Prolonged membrane performance of tube B, single gas permeance (presented data obtained at $T = 250\,^{\circ}C$, $\Delta p = 3.9$ bar).

longer duration of exposure. The data acquired in the long-term measurement indicates that the high performance of the membranes can be maintained for more than 2100 h at these conditions.

4. Conclusions

High performance micro-porous silica membranes have been coated on the inside of tubular supports up to 55 cm long, with an improved surface morphology. The performance of these membranes is reproducible and compares favorably with the performance of low surface area flat plate and short tubular (10 cm) membranes. At 250 °C and a pressure difference of 2 bar the 55 cm long tubular membranes display hydrogen permeance in the range $(0.5–1) \times 10^{-6}$ mol m^{-2} s^{-1} Pa^{-1}, and permselectivity of hydrogen with respect to methane in the range 350–400. At $\leq$350 °C, no significant changes in the permeance and permselectivity have been observed over a period of more than 2100 h.

The present method allows straightforward and reproducible coating of large surface area high performance silica membranes, and can be anticipated to be beneficial for commercial application of these membranes.

References

[1] B.-K. Sea, K. Watanabe, K. Kusakabe, S. Morooka, S.-S. Kim, Formation of hydrogen permselective silica membrane for elevated temperature hydrogen recovery from a mixture containing steam, Gas Sep. Purif. 10 (1996) 187.
[2] G.-J. Hwang, J.-W. Kim, H.-S. Choi, K. Onuku, Stability of a silica membrane prepared by CVD using [gamma]- and [alpha]-alumina tube as the support tube in the HI–H_2O gaseous mixture, J. Membr. Sci. 215 (2003) 293.
[3] S. Gopalakrishnan, M. Nomura, T. Sugawara, S.-I. Nakao, Preparation of a multi-membrane module for high-temperature hydrogen separation, Desalination 193 (2006) 230.
[4] Y. Gu, P. Hacarlioglu, S.T. Oyama, Hydrothermally stable silica–alumina composite membranes for hydrogen separation, J. Membr. Sci. 310 (2008) 28.
[5] T. Tsuru, T. Morita, H. Shintani, T. Yoshioka, M. Asaeda, Membrane reactor performance of steam reforming of methane using hydrogen-permselective catalytic SiO_2 membranes, J. Membr. Sci. 316 (2008) 53.
[6] M. Asaeda, S. Yamasaki, Separation of inorganic/organic gas mixtures by porous silica membranes, Sep. Purif. Technol. 25 (2001) 151.
[7] K. Kusakabe, F. Shiboa, G. Zhao, K.-I. Sotowa, K. Watanabe, T. Saito, Surface modification of silica membranes in a tubular-type module, J. Membr. Sci. 215 (2003) 321.
[8] T.A. Peters, J. Fontalvo, M.A.G. Vorstman, N.E. Benes, R.A. van Dam, Z.A.E.P. Vroon, E.L.J. van Soest-Vercammen, J.T.F. Keurnetjes, Hollow fibre microporous silica membranes for gas separation and pervaporation: synthesis, performance and stability, J. Membr. Sci. 248 (2005) 73.
[9] Y. Yoshino, S. Takehiro, B.N. Nair, H. Taguchi, N. Itoh, Development of tubular substrates, silica based membranes and membrane modules for hydrogen separation at high temperature, J. Membr. Sci. 267 (2005) 8.
[10] M.K. Koukou, N. Papayannakos, N.C. Markatos, M. bracht, H.M. van Veen, A. Roskam, Performance of ceramic membranes at elevated pressure and temperature: effect of non-ideal flow conditions in a pilot scale membrane separator, J. Membr. Sci. 155 (1999) 241.
[11] C.-Y. Tsai, C.-Y. Tam, Y. Lu, C.J. Brinker, Dual-layer asymmetric microporous silica membranes, J. Membr. Sci. 169 (2000) 255.
[12] K. Yoshida, Y. Hirano, H. Fujii, T. Tsuru, M. Asaeda, Hydrothermal stability and performance of silica–zirconia membranes for hydrogen separation in hydrothermal conditions, J. Chem. Eng. Jpn. 34 (2001) 523.
[13] A. Nijmeijer, H.K. Rune Bredesen, H. Verweij, Preparation and properties of hydrothermally stable gamma alumina membranes, J. Eur. Ceram. Soc. 84 (2001) 136.
[14] A. Nijmeijer, Hydrogen-Selective Silica Membranes for Use in Membrane Steam Reforming, 1st ed., Print Partners Ipskamp, Enschede, 1999.
[15] R.M. de Vos, High-Selectivity, High-Flux Silica Membranes for Gas Separation, 1st ed., Print Partners Ipskamp, Enschede, 1998.
[16] R.M. de Vos, H. Verweij, Improved performance of silica membranes for gas separation, J. Membr. Sci. 143 (1998) 37.
[17] C.J. Brinker, G.W. Scherer, Sol–Gel Science: The Physics and Chemistry of Sol–Gel Processing, Academic Press, London, 1990.
[18] S.F. Kistler, P.M. Scheizer, Liquid Film Coating, 1st ed., Chapman & Hall, Cambridge, 1997.